

# Role of TRH/UCN3 neurons of the perifornical area/bed nucleus of stria terminalis region in the regulation of the anorexigenic POMC neurons of the arcuate nucleus in male mice and rats

Zoltán Péterfi<sup>1</sup> · Erzsébet Farkas<sup>1,2</sup> · Kata Nagyunyomi-Sényi<sup>1</sup> · Andrea Kádár<sup>1</sup> · Szenci Ottó<sup>3,4</sup> · András Horváth<sup>3,4</sup> · Tamás Füzesi<sup>1</sup> · Ronald M. Lechan<sup>5,6</sup> · Csaba Fekete<sup>1,5</sup> 

Received: 4 June 2017 / Accepted: 17 October 2017 / Published online: 9 November 2017  
© Springer-Verlag GmbH Germany 2017

**Abstract** Two anorexigenic peptides, thyrotropin-releasing hormone (TRH) and urocortin 3 (UCN3), are co-expressed in a continuous neuronal group that extends from the perifornical area to the bed nucleus of stria terminalis, raising the possibility that this cell group may be involved in the regulation of energy homeostasis. In this study, therefore, we tested the hypothesis that the TRH/UCN3 neurons regulate food intake by influencing feeding-related neuropeptide Y (NPY) and/or proopiomelanocortin (POMC) neurons in the arcuate nucleus (ARC). Triple-labeled immunofluorescent preparations demonstrated that only very few NPY neurons ( $4.3 \pm 1.3\%$ ) were contacted by double-labeled TRH/UCN3 axons in the ARC. In contrast, more than half of the POMC neurons ( $52.4 \pm 8.5\%$ )

were contacted by double-labeled axons. Immuno-electron microscopy demonstrated that the UCN3 axons established asymmetric synapses with POMC neurons, indicating the excitatory nature of these synaptic specializations. Patch clamp electrophysiology revealed that TRH and UCN3 have antagonistic effects on the POMC neurons. While UCN3 depolarizes and increases the firing rate of POMC neurons, TRH prevents these effects of UCN3. These data demonstrate that TRH/UCN3 neurons in the perifornical/BNST region establish abundant synaptic associations with the POMC neurons in the ARC and suggest a potentially important role for these neurons in the regulation of food intake through an antagonistic interaction between TRH and UCN3 on the electrophysiological properties of POMC neurons.

Zoltán Péterfi and Erzsébet Farkas equally contributed to the work.

✉ Csaba Fekete  
fekete.csaba@koki.mta.hu

- <sup>1</sup> Department of Endocrine Neurobiology, Institute of Experimental Medicine, Hungarian Academy of Sciences, Szigony u. 43, Budapest 1083, Hungary
- <sup>2</sup> Multidisciplinary Doctoral School of Sciences and Technology, Pázmány Péter Catholic University, Budapest 1083, Hungary
- <sup>3</sup> Department and Clinic for Production Animals, University of Veterinary Medicine, Üllő, Dóra Major, Budapest 2225, Hungary
- <sup>4</sup> BMTA–SZIE Large Animal Clinical Research Group, Dóra Major, Üllő 2225, Hungary
- <sup>5</sup> Department of Medicine, Division of Endocrinology, Diabetes and Metabolism, Tupper Research Institute, Tufts Medical Center, Boston, MA 02111, USA
- <sup>6</sup> Department of Neuroscience, Tufts University School of Medicine, Boston, MA 02111, USA

**Keywords** Thyrotropin-releasing hormone · Urocortin 3 · Proopiomelanocortin · Arcuate nucleus · Perifornical region · Bed nucleus of stria terminalis · Antagonist effect

## Introduction

Thyrotropin-releasing hormone (TRH) is well known as a hypophysiotropic hormone regulating the hypothalamic–pituitary–thyroid axis (Fekete and Lechan 2014). In addition to this function, however, TRH also serves as a neurotransmitter in the central nervous system regulating a number of physiologic processes, including food intake, gut motility, arousal and blood pressure (Fekete and Lechan 2014). TRH has a potent anorexigenic effect when it is administered centrally (Lechan and Fekete 2006), but currently, little information is known about the TRH cell population that regulates food intake. Urocortin 3 (UCN3), another anorexigenic peptide (Fekete et al. 2007), is

present in the majority of TRH neurons in the perifornical region of the hypothalamus (Wittmann et al. 2009). A smaller group of TRH/UCN3 neurons are present in the bed nucleus of stria terminalis (BNST). These two neuronal populations appear to form a continuous neuronal group. The presence of two anorexigenic peptides in this neuronal population raised the possibility that TRH/UCN3 neurons may be involved in the regulation of food intake. The hypothesis was also supported by evidence that perifornical TRH/UCN3 neurons have a major projection into the arcuate nucleus (ARC) (Wittmann et al. 2009) where both anorexigenic and orexigenic neuronal groups are located (Schwartz et al. 2000).

Neurons containing the orexigenic peptides, neuropeptide Y (NPY) and agouti-related protein (AGRP) are located in the ventromedial part of the ARC (Schwartz et al. 2000), while neurons containing the anorexigenic proopiomelanocortin (POMC) are present in the lateral part of the nucleus (Schwartz et al. 2000). Both neuronal groups are regulated by peripheral feeding-related hormones, such as leptin, insulin, ghrelin and glucocorticoids, and have critical roles in the regulation of energy homeostasis (Schwartz et al. 2000; Gropp et al. 2005; Luquet et al. 2005).

To determine whether the TRH/UCN3-expressing neurons in the perifornical/BNST region regulate food intake via projections to feeding-related neuronal groups in the ARC, we studied whether the TRH/UCN3 neurons innervate NPY and/or POMC neurons in the ARC and determined the effects of these peptides on POMC neurons using patch clamp electrophysiology.

## Materials and methods

### Animals

The neuroanatomical experiments were carried out on adult, male, Wistar rats (TOXI-COOP KKT, Budapest, Hungary), weighing 250–300 g and adult male CD1 mice weighing 25–30 g (from the breeding colony of the Institute of Experimental Medicine of the Hungarian Academy of Sciences). To identify the POMC neurons in *in vitro* slices, the *in vitro* patch clamp electrophysiology studies were performed using adult (age 40–80 days) male POMC/*Cre//Gt(ROSA)26Sor\_CAG/tdTomato//C57Bl/6 J* mice. These mice were generated by crossing homozygous *Tg(Pomc1-cre)16Low1/J* mice (Jackson Laboratories) with homozygous *Gt(ROSA)26Sor\_CAG/LSL\_tdTomato (Tm)* mice (Jackson Laboratories). The resulting double, transgenic mice express the red fluorescent *tdTomato* exclusively in POMC neurons. The animals were housed under standard environmental conditions (light between 06:00

and 18:00 h, temperature  $22 \pm 1$  °C, rat chow and water were available *ad libitum*). All experimental protocols were reviewed and approved by the Animal Welfare Committee at the Institute of Experimental Medicine of the Hungarian Academy of Sciences.

### Generation of rat anti-mouse proTRH 178-200 and sheep anti-POMC sera

To study the relationship between TRH/UCN3 axons and the POMC neurons in the ARC of mice, we generated antisera against mouse proTRH 178-200 (sequence: H-FIDPELQRSWEETEGEEGLMPE-NH<sub>2</sub>) in rats, and against POMC (sequence: H-W(C1)LESSQ(C2)QDLSTESNLLA(C2)IRA(C1)KPK(Aoa)-NH<sub>2</sub>).

The mouse proTRH fragment (4 mg) was conjugated to 25 mg thyroglobulin (Sigma) with 12 mg EDCI in 2 ml 2{N-Morpholino}ethansulfonic acid (MES) buffer, pH 4.7. The mixture was kept at room temperature for 3 h and dialyzed against phosphate buffered saline (PBS). For initial immunization, 250 µg TRH-thyroglobulin complex was dissolved in 0.5 ml PBS, emulsified with an equal volume of Freund's complete adjuvant (Sigma) and injected subcutaneously to rats. Subsequent boosts with Freund's incomplete adjuvant were administered at 21-day intervals. Eight days after the fifth immunization, the rats were decapitated and trunk blood was collected. The serum was separated by centrifugation.

The POMC immunogen complex was prepared by gently mixing 25 mg thyroglobulin (Sigma) dissolved in phosphate buffer (PB), pH 6.5 and 0.2 mg S-4FB dissolved in DMSO. The mixture was kept at 37 °C for 4 h, and then dialyzed for 30 min against PB, pH 6.5, four times. Four micrograms of POMC peptide dissolved in PBS, pH 6.0, was added to the carrier-linker mixture and stirred at room temperature overnight. Finally, the conjugate was dialyzed against PBS. For initial immunization, 2000 µg POMC-S-4FB-thyroglobulin complex was dissolved in 0.5 ml PBS, emulsified with an equal volume of Freund's complete adjuvant (Sigma) and injected subcutaneously into sheep. Subsequent boosts with Freund's incomplete adjuvant were administered at 28-day intervals. Eight days after the fourth immunization, blood was collected and the serum was separated by centrifugation.

### Animal preparation and fixation for immunocytochemistry

Rats anesthetized with a mixture of ketamine and xylazine (ketamine 50 mg/kg, xylazine 10 mg/kg body weight, ip) were injected intracerebroventricularly with 100 µg colchicine in 5 µl 0.9% saline under stereotaxic control to facilitate the visualization of peptides in perikarya in the

ARC. Twenty hours later, the animals were anesthetized as described above and perfused transcardially with 20 ml 0.01 M PBS pH 7.4, followed by 150 ml mixture of 1% acrolein and 3% paraformaldehyde in 0.1 M PB pH 7.4. The brains were rapidly removed. For light microscopy ( $n = 3$ ), the brains were cryoprotected in 30% sucrose in 0.01 M PBS overnight at room temperature. For electron microscopy ( $n = 3$ ), the brains were postfixed in 4% paraformaldehyde in 0.1 M PB overnight at 4 °C.

Mice were anesthetized with a mixture of ketamine and xylazine (ketamine 50 mg/kg, xylazine 10 mg/kg body weight, i.p.) and perfused transcardially with 10 ml 0.01 M PBS, pH 7.4, followed by 50 ml 4% paraformaldehyde in 0.1 M PB pH 7.4. The brains were rapidly removed and cryoprotected in 30% sucrose in 0.01 M PBS overnight at room temperature.

### Tissue preparation for triple-labeling immunofluorescence

Serial, 25  $\mu$ m thick coronal sections through the ARC of rats were cut on freezing microtome (Leica). The sections were pretreated with 1% sodium borohydride in distilled water for 30 min, washed in PBS and then pretreated with 0.5% Triton X-100 and 0.5% H<sub>2</sub>O<sub>2</sub> in 0.01 M PBS for 15 min. Nonspecific antibody binding was blocked by treatment with 2% normal horse serum (NHS) in PBS for 15 min.

Mouse tissues were treated similarly, but the sodium borohydride treatment was omitted.

### Triple-labeling immunofluorescence for TRH, UCN3 and $\alpha$ -MSH or NPY in rats

One-in-four series of sections from each brain were incubated in rabbit anti-UCN3 serum at 1:60,000 dilution, preabsorbed with 75  $\mu$ g/ml rat CRF (Bachem), mouse anti-TRH serum at 1:4000 and either sheep anti- $\alpha$ -MSH serum at 1:20,000 or sheep anti-NPY serum at 1:8000 for 2 days at 4 °C. Then, sections were treated with biotinylated donkey anti-rabbit IgG at 1:500 (Jackson) for 2 h, followed by the ABC at 1:1000 for 2 h. After washes in PBS, the sections were subjected to biotinylated tyramide signal amplification using the TSA amplification kit (Perkin Elmer Life and Analytical Sciences, Waltham, MA) according to the manufacturer's description. After further washes, the sections were incubated in a mixture of Fluorescein DTAF-conjugated Streptavidin (1:300, Jackson), Alexa 555-conjugated donkey anti-mouse IgG (1:500, Jackson) and Cy5-conjugated donkey anti-sheep IgG (1:100, Jackson) for 2 h, mounted onto glass slides and coverslipped with Vectashield mounting medium (Vector).

### Triple-labeling immunofluorescence for TRH, UCN3 and POMC in mice

One-in-four series of sections from each brain were incubated in a mixture of rabbit anti-UCN3 serum at 1:60,000 dilution preabsorbed with 75  $\mu$ g/ml rat CRF (Bachem), sheep anti-POMC serum at 1:5000 and rat anti-TRH serum at 1:500 dilution overnight at room temperature. Then, the sections were incubated in a mixture of Alexa 555-conjugated donkey anti-rabbit IgG (1:250, Jackson), Dylight 405-conjugated donkey anti-sheep IgG (1:250, Jackson) and Alexa 488-conjugated donkey anti-rabbit IgG (1:250, Jackson) for 2 h, mounted onto glass slides and coverslipped with Vectashield (Vector) mounting medium.

### Image analyses

Images were taken using Bio-Rad Radiance 2000 confocal microscope (Bio-Rad Laboratories, Hemel Hempstead, UK) using line by line sequential scanning with laser excitation lines 488 nm for Fluorescein DTAF and Alexa Fluor 488 and 543 nm for Alexa Fluor 555; beamsplitter/emission filters, 560/500–530 nm for Fluorescein DTAF and Alexa Fluor 488 and 560–625 nm for Alexa Fluor 555. For 40 $\times$  and 60 $\times$  oil lenses, pinhole sizes were set to obtain optical slices of 1 and 0.8  $\mu$ m thickness, respectively, and the series of optical sections were recorded with 1.0 and 0.5  $\mu$ m Z steps.

Images were analyzed with Laser Vox (Bio Rad Laboratories, Hemel Hempstead, UK) and with Image pro plus softwares (Media Cybernetics Inc., Bethesda MD).

Z-stack images of the entire ARC of every fourth 25  $\mu$ m thick section from three brains were taken by confocal microscopic imaging using a 40X objective and 1.0  $\mu$ m Z steps. The Z-stacks covered the entire depth of the sections. Each NPY- or  $\alpha$ -MSH-immunoreactive (IR) neuron was followed through the Z-stack images, and immunoreactive axon varicosities were sought on the surface of the perikaryon and primary dendrites of these cells. A varicosity was considered to establish juxtaposition with the neuron if a gap was not observed between the cell and the varicosity. The number of UCN3 and TRH/UCN3 contacts on all NPY- and  $\alpha$ -MSH-immunoreactive (IR) neurons, and the number of contacted neurons were counted. Data are presented as mean  $\pm$  SEM.

### Ultrastructural double-labeling immunocytochemistry for UCN3 and $\alpha$ -MSH

Serial, 50  $\mu$ m thick coronal sections were cut on a Leica VT 1000S vibratome (Leica Microsystems, Wetzlar, Germany) through the ARC. The sections were first pretreated

in 1% sodium borohydride in 0.01 M PBS for 30 min, washed in 0.01 M PBS and then treated with 0.5% H<sub>2</sub>O<sub>2</sub> in 0.01 M PBS for 15 min. The sections were cryoprotected in 15% sucrose in 0.01 M PBS for 15 min at room temperature and in 30% sucrose in 0.01 M PBS overnight at 4 °C and then, quickly frozen over liquid nitrogen and thawed three times to improve antibody penetration into the tissue.

The pretreated sections were placed in a mixture of sheep anti- $\alpha$ -MSH serum (1:1000) and rabbit anti-UCN3 serum (1:1000) preabsorbed with 75  $\mu$ g/ml rat CRF (Bachem) for 4 days at 4 °C. After rinsing in 0.01 M PBS and 0.1% cold water fish gelatin/1% bovine serum albumin (BSA) in PBS, the sections were incubated in donkey anti-sheep IgG conjugated with 0.8 nm colloidal gold (Electron Microscopy Sciences, Fort Washington, PA) diluted at 1:100 and biotinylated donkey anti-rabbit IgG diluted at 1:500 in 0.01 M PBS containing 0.1% cold water fish gelatin and 1% BSA. After washing, the sections were fixed in 1.25% glutaraldehyde in 0.1 M PB for 10 min at room temperature. After further rinsing in 0.01 M PBS, the sections were washed in Aurion ECS buffer (Aurion) (1:10) diluted in distilled water. The gold particles were silver intensified with the Aurion R-Gent SE-LM Kit after rinsing in 0.2 M sodium citrate, pH 7.5, followed by treatment in ABC (1:1000). UCN3-immunoreactivity was detected with 0.05% DAB/0.15% Ni-ammonium-sulfate/0.005% H<sub>2</sub>O<sub>2</sub> in 0.05 M Tris buffer, pH 7.6.

Sections were osmicated, and then treated with 2% uranyl acetate in 70% ethanol for 30 min. Following dehydration in an ascending series of ethanol and propylene oxide, the sections were flat embedded in Durcupan ACM epoxy resin (Fluka) on liquid release agent (Electron Microscopy Sciences)-coated slides, and polymerized at 56 °C for 2 days.

After polymerization, 60–70 nm ultrathin sections were cut with a Leica ultracut UCT ultramicrotome (Leica Microsystems, Wetzlar, Germany). Sections were mounted onto Formvar-coated single slot grids, contrasted with 2% lead citrate and examined with a Jeol-100 C transmission electron microscope.

### Antibody characterization and specificity of the method

The used antibodies are summarized in Table 1. The specificity of rabbit antiserum against UCN3 (Wittmann et al. 2009), mouse antisera against TRH (Sarvari et al. 2012), sheep antiserum against NPY (Wittmann et al. 2002) and sheep antiserum against  $\alpha$ -MSH (Elias et al. 1998) was previously described.

To determine the specificity of the rat anti-mouse proTRH 178-200 antiserum, double-labeling

immunofluorescence was performed using the rat anti-mouse proTRH 178-200 antiserum and sheep TRH antiserum (Wittmann et al. 2009). The staining pattern with the two antibodies showed complete colocalization. Immunostaining with the sheep POMC antiserum resulted in an identical distribution of the immunoreactive structures as was observed with the rabbit anti-POMC antiserum [Phoenix Pharmaceuticals, (Wittmann et al. 2013)]. Omission of TRH or UCN3 primary antisera resulted in a complete loss of colocalization of the two peptides.

### Slice preparation for electrophysiological recordings

Mice were deeply anesthetized with isoflurane and subsequently decapitated. Brains were quickly removed from the skull and placed into ice-cold, cutting solution (composition in mM: 87 NaCl, 2.5 KCl, 7 MgCl<sub>2</sub>, 1.25 NaH<sub>2</sub>PO<sub>4</sub>, 0.5 CaCl<sub>2</sub>, 15 glucose, 75 sucrose, pH 7.4; 280–300 mOsm/L) saturated with 95% O<sub>2</sub> and 5% CO<sub>2</sub> (carbogen gas). Hypothalamic blocks were dissected from the brains and 200- $\mu$ m-thick coronal slices were prepared using VT1200S vibratome (Leica). Then, the slices were bisected along the third ventricle and transferred into a holding chamber containing artificial cerebrospinal fluid (ACSF) with the following composition (in mM): 126 NaCl, 2.5 KCl, 1.25 NaH<sub>2</sub>PO<sub>4</sub>, 2 MgCl<sub>2</sub>, 2.4 CaCl<sub>2</sub>, 26 NaHCO<sub>3</sub> and 10 glucose, saturated with carbogen gas (pH 7.4; 280–300 mOsm/L) at 36 °C, then allowed to cool at room temperature for at least 1.5 h before the recording. Slices were transferred to a submersion type of recording chamber containing ACSF or ACSF and 660 nM tetrodotoxin (TTX). The recordings were performed at 32–33 °C and the flow rate was between 1.5 and 2 ml/min.

### Whole-cell clamp recording

POMC neurons were identified in the ARC based on the red fluorescence of tdTomato, and were measured using current clamp configuration in whole-cell patch clamp mode. The instruments used for data recording were as follows: Multiclamp 700B patch clamp amplifier, Digidata-1440A data acquisition system and pCLAMP 10.4 software (Axon Instruments-Molecular Devices Co.). The headstage of the amplifier was fitted to a Luigs&Neumann SM7 micromanipulator system. The cells were visualized by an Eclipse FN1 upright microscope (Nikon) equipped with infrared-DIC optics. The patch electrodes (OD = 1.5 mm, thin wall, Garner Co.) were pulled with a Flaming-Brown P-97 horizontal puller (Sutter Instrument Co.). Resistance of the patch electrodes was 3–5 M $\Omega$ . The intracellular recording solution had the following composition (in mM): 110 K-gluconate, 4 NaCl, 20 HEPES, 0.1 EGTA, 10

phosphocreatine di(tris) salt, 2 ATP, 0.3 GTP (pH 7.25; 280–300 mOsm/L). Whole-cell patch clamp recordings were filtered at 3 kHz using the built-in Bessel filter of the amplifier and digitized at 15 kHz. In current clamp recordings, holding potential was set at  $-60$  mV to test passive membrane properties or  $I = 0$  configuration test membrane potential changes. Unless otherwise stated, the chemicals for the intracellular and extracellular solutions were purchased from Sigma-Aldrich; TRH (bath application: 1 or 5  $\mu$ M) and UCN3 (bath application: 100 nM) were purchased from Bachem (Switzerland). The CRF<sub>2</sub> receptor antagonist, K41498 (bath application: 1  $\mu$ M), were purchased from Tocris Bioscience (Germany).

### Experimental protocol of whole-cell patch clamp experiments

As a first step, we studied the effects of TRH, UCN3 and the combination of the two peptides (TRH + UCN3) on spontaneous firing activity of the POMC neurons. In addition, the passive and active membrane properties of these neurons were measured in response to the different peptide treatments. The red fluorescent, tdTomato-expressing POMC neurons were visualized under epifluorescent illumination using the following filter set: Chroma (USA), excitation: 556/20 nm, emission: 609/54 nm. The cells were detected with a high resolution Zyla CCD camera (ANDOR). After identification of POMC neurons, the illumination was switched to bright-field illumination and the cells were detected by infrared Nomarski differential interference contrast optics. After establishing stable, whole-cell, patch clamp connection with POMC-positive neurons, the resting membrane potential was first measured. Then, in each series of experiments, a control period (2–3 min) was recorded, which was followed by a drug treatment phase (5–10 min). For recordings of the spontaneous firing properties, POMC neurons were recorded in  $I = 0$  configuration. To determine the passive and active membrane properties, POMC neurons were studied in current clamp configuration, and a step-protocol (steps: 400 ms long) was applied starting at  $-60$  mV and increased by 5 mV steps.

To determine whether the observed effects of TRH and UCN3 were exerted directly on POMC neurons, the experiments were repeated on synaptically isolated POMC neurons after adding TTX (660 nM) into the ACSF solution. In these experiments, the effects of TRH, UCN3 or the combination of the two peptides (TRH + UCN3) were studied on the membrane potential (MP) and passive membrane properties of the POMC neurons. During the control period, first the passive membrane properties of the cell were measured in current clamp configuration by injecting  $-20$  pA for a 400 ms period at the holding

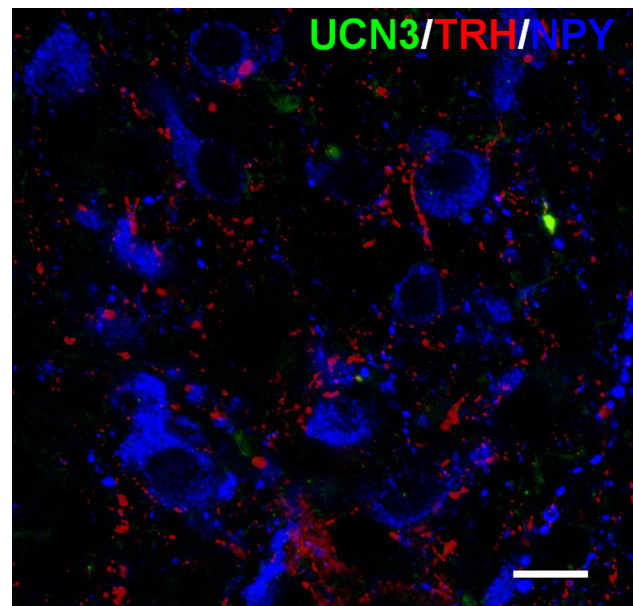


**Fig. 1** Relationship between TRH/UCN3 axons and NPY neurons in the ARC of rats. Triple-labeled immunofluorescent detection of the UCN3—(green), TRH—(red) immunoreactive (IR) axons and NPY—(blue) neurons in the ARC. Only scattered double-labeled axons can be observed around the NPY neurons in ventromedial part of the ARC. Scale bar = 10  $\mu$ m

potential ( $-60$  mV), followed by the measurement of the membrane potential (MP) during control conditions in  $I = 0$  configuration. After bath application of different drugs, the measurements were repeated in the same sequence as during the control condition to determine the treatment effects.

### Statistical analysis of in vitro measurements

Membrane potentials and passive membrane properties were analyzed offline using the Clampfit module of the PClamp 10.4 software (Molecular Devices). All data for each experiment were reported as mean  $\pm$  standard error of the mean (SEM). Data were analyzed using paired  $t$  test (treatment values compared to their own control period). No significant differences were observed among the control values of the POMC neurons used for different peptide treatments by one-way analysis of variance (ANOVA). An  $\alpha$ -level of  $P < 0.05$  was regarded as statistically significant.

## Results

### TRH/UCN3 neurons of the perifornical/BNST region innervate POMC neurons in the ARC

Since we previously demonstrated that colocalization of TRH and UCN3 occurs almost exclusively in the

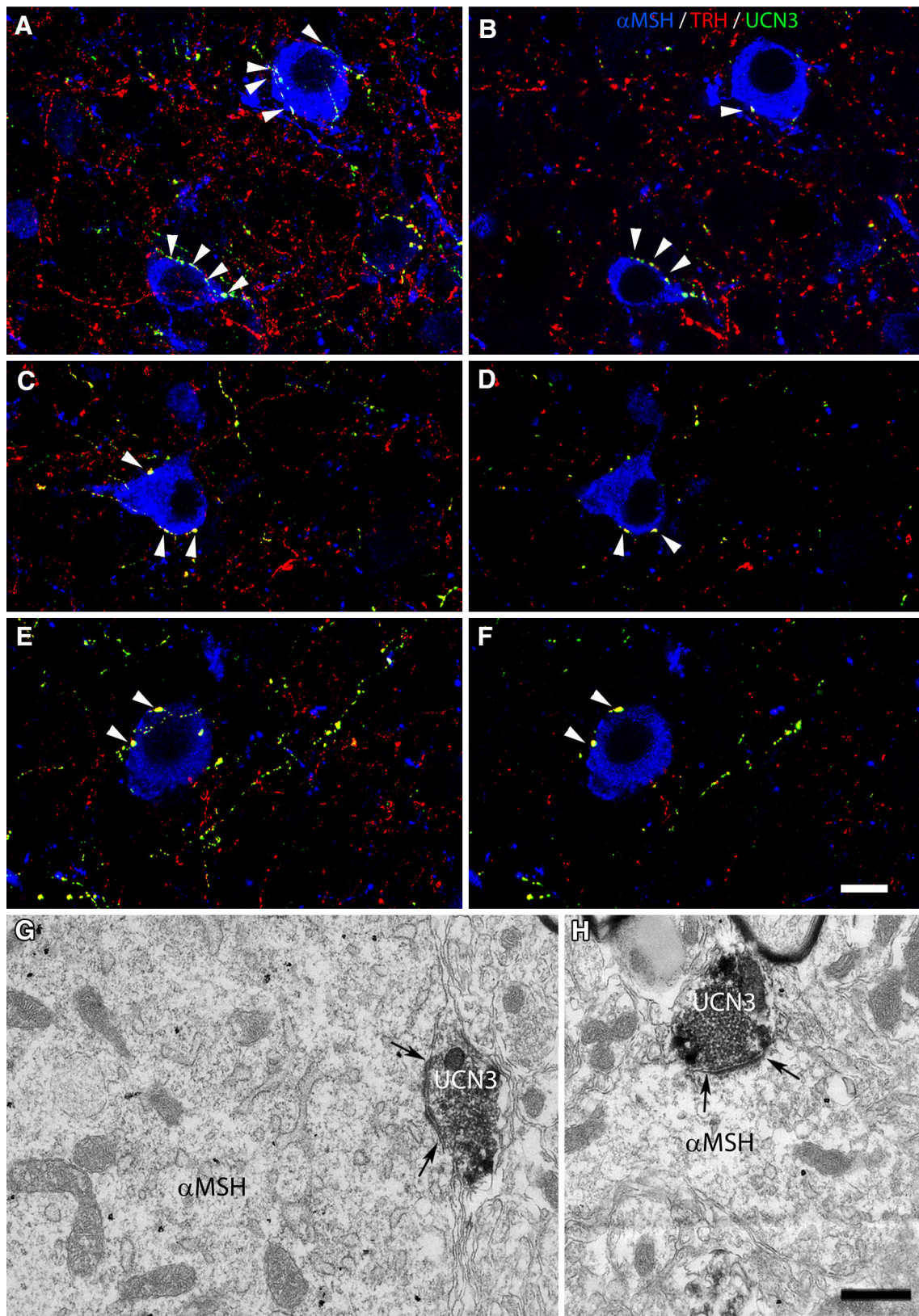


**Fig. 2** Relationship between TRH/UCN3 axons and POMC neurons in the ARC of rats. Triple-labeled immunofluorescent detection of the UCN3—(green), TRH—(red) immunoreactive (IR) axons  $\alpha$ -MSH—(blue) neurons in the ARC of rats (**a–f**). The TRH/UCN3 axons (yellow) contacted approximately half of the  $\alpha$ -MSH neurons in the lateral part of ARC. Arrows point to the double-labeled axon varicosities on the surface of  $\alpha$ -MSH neurons. **a, c** and **e** represent projections of 24 (**a**) or 8 (**b** and **e**) 0.8  $\mu$ m thick optical slices, while **b, d** and **f** show a single 0.8  $\mu$ m thick optical slice. Electron micrographs (**g, h**) illustrate synaptic associations (arrows) between  $\alpha$ -MSH-IR neurons and UCN3-IR terminals in the ARC. The  $\alpha$ -MSH-IR perikarion (**g**) and dendrite (**h**) are labeled with highly electron dense gold–silver granules, while the UCN3-IR terminals are recognized by the presence of the electron dense DAB chromogen. Asymmetric type synapses were observed between UCN3-IR axon varicosities and the  $\alpha$ -MSH-IR profiles. Arrows (**g, h**) point to the synapses. Nu, nucleus; Scale bar on (**f**) = 20  $\mu$ m and corresponds to (**a–f**); scale bar on (**h**) = 0.25  $\mu$ m and corresponds to (**g, h**)

perifornical/BNST region (Wittmann et al. 2009), the colocalization of TRH and UCN3 was used as a marker for axons originating from perifornical/BNST TRH/UCN3 neurons. TRH/UCN3-IR axons were primarily observed in the lateral part of the ARC, while a dense network of TRH-IR axons was observed throughout the entire ARC. The vast majority of UCN3-IR axons contained TRH-immunoreactivity in this nucleus. However, a large portion of TRH-IR axons did not contain UCN3. Double-labeled TRH/UCN3 axons were primarily located in the lateral part of the ARC.

NPY-IR neurons primarily occupied the medial part of the ARC where only scattered TRH/UCN3 axons were found (Fig. 1). TRH/UCN3-IR axon terminals were observed in juxtaposition to only  $4.3 \pm 1.3\%$  of NPY-IR neurons. An average of  $1.7 \pm 0.2$  TRH/UCN3 axon varicosities were observed on the surface of the contacted NPY

neurons. In contrast, there was a large overlap of double-labeled TRH/UCN3-IR axons with  $\alpha$ -MSH-containing neurons in the lateral ARC (Fig. 2a–f). Indeed, more than half ( $52.4 \pm 8.5\%$ ) of the  $\alpha$ -MSH-containing neurons were contacted by TRH/UCN3-IR axon terminals. The average number of TRH/UCN3 axon varicosities per contacted  $\alpha$ -MSH neurons was  $6.5 \pm 0.8$ .

Since the vast majority ( $88.1 \pm 1.2\%$ ) of UCN3-IR axon varicosities on the surface of  $\alpha$ -MSH-IR neurons also co-contained TRH-immunoreactivity, UCN3-immunoreactivity was used for the ultrastructural studies to identify UCN3 axons derived from the perifornical/BNST region. UCN3-IR axon terminals labeled with nickel-intensified DAB formed synaptic contacts with the silver-intensified immunogold-labeled  $\alpha$ -MSH-IR perikarya and dendrites (Fig. 2g, h). All observed synapses between these two systems were of the asymmetric type.

Triple-labeling immunofluorescence for UCN3, TRH and POMC on hypothalamic sections of mice demonstrated that, similarly to rats, the double-labeled UCN3/TRH axons concentrated in the lateral part of the ARC and the POMC neurons in this nucleus also received TRH/UCN3-containing contacts (Fig. 3).

### Effect of TRH and UCN3 on the electrophysiological properties of POMC neurons in the ARC

To determine how the two, anorexigenic peptides influence POMC neurons, the effects of TRH, UCN3, and the combination of the two peptides were studied on the electrophysiological properties of these neurons. The resting membrane potential of POMC neurons immediately after breaking the plasma membrane was an average –

**Table 1** Antibody description

Peptide/protein target	Antigen sequence	Source	Manufacturer, catalog #	Species raised in; monoclonal or polyclonal	Dilution used
POMC	H-W(C1)LESSQ(C2) QDLSTESNLLA(C2)IRA (C1)KPK(Aoa)-NH <sub>2</sub>	Generated in our laboratory		Sheep polyclonal	1:5000
TRH	pEHP-NH <sub>2</sub>	Generated in our laboratory	08W2	Sheep polyclonal	1:50000
TRH	pEHP-NH <sub>2</sub>	Generated in our laboratory		Mouse polyclonal	1:1000
TRH	H-FIDPELQRSWEETEGEEGLMPE-NH <sub>2</sub>	Generated in our laboratory	2/3/c	Rat polyclonal	1:500
Human UCN3	YGPHKFYKAKPIFSLNTAL	Gift from Wylie Vale	PBL #6570	Rabbit polyclonal	1:60000
NPY	YPSKPDNPGEDAPAEDMARY YSALRHYINLITRQRY	Gift from Istvan Merchenthaler		Sheep polyclonal	1:8000
$\alpha$ -MSH	Ac-SYSMEHFRWGKPV-NH <sub>2</sub>	Gift from Jeffrey B Tatro	BA387	Sheep polyclonal	1:20000

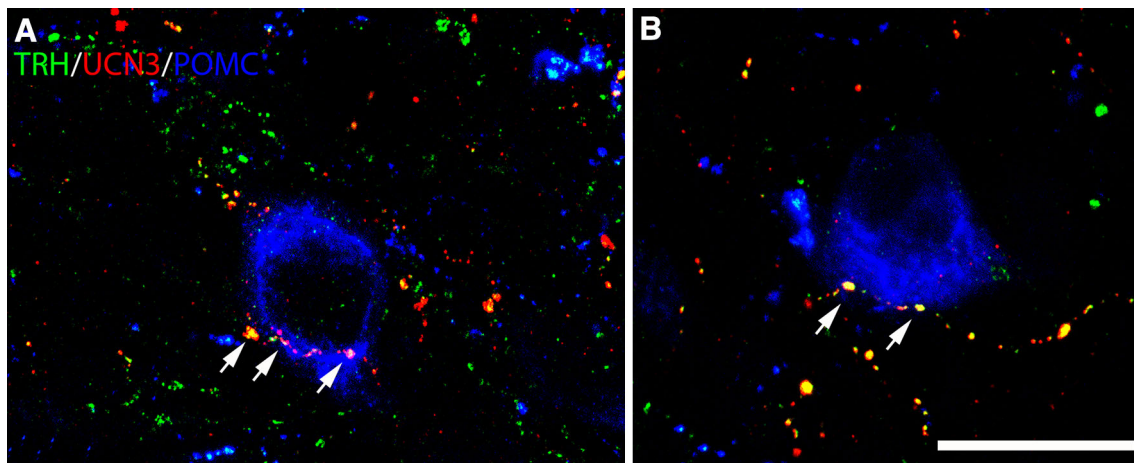


**Fig. 3** Relationship between TRH/UCN3 axons and POMC neurons in the ARC of mice. Triple-labeled immunofluorescent detection of the UCN3—(red), TRH—(green) immunoreactive (IR) axons and

POMC—(blue) neurons in the ARC. Double-labeled TRH/UCN3-IR axon varicosities (arrows) were observed in juxtaposition to POMC neurons (a, b). Scale bar = 20  $\mu$ m

$54.0 \pm 1.2$  mV ( $n = 83$ ). Administration of TRH hyperpolarized the membrane potential of POMC neurons ( $p = 0.0017$ ) and significantly decreased the spontaneous spike frequency (Fig. 4) of these cells ( $p = 0.009$ ) when compared to the control values of the same cell (Table 2). In contrast, UCN3 treatment, markedly depolarized the membrane potential (Table 2), ( $p = 0.001$ ) and caused a robust increase of the spontaneous spike frequency of POMC neurons ( $p = 0.0005$ ) (Fig. 4). Although the combination of TRH and UCN3 treatment did not significantly alter the membrane potential compared to the control values, it decreased the spontaneous spike frequency ( $p = 0.024$ ). No treatment influenced the amplitude of the spontaneous spikes (Table 2).

Next, we elucidated specific changes of the passive membrane properties of the POMC—expressing neurons under different treatment conditions. TRH did not significantly affect the input resistance of these neurons (Table 2), but UCN3 alone or together with TRH significantly affected this parameter ( $p = 0.04$ ;  $p = 0.02$ , respectively). Neither the membrane time constants nor membrane capacitance (Table 2) were significantly affected by any of the treatments compared to their controls.

When active membrane properties of the POMC neurons were studied (Table 2), TRH decreased the AP firing frequency ( $p = 0.01$ ) and increased the inter-spike interval (Table 2). In addition, TRH increased the amount of current that was necessary to initiate the first spike (rheobase;  $p = 0.03$ ). TRH did not influence other measured parameters of POMC neurons. UCN3 treatment increased the AP firing frequency ( $p = 0.005$ ) and accommodation ratio ( $p = 0.01$ ), while it decreased the rheobase ( $p < 0.001$ ) when treatment values were compared to the control values (Table 2). Cotreatment of POMC neurons with both TRH

and UCN3 caused similar effects compared to TRH treatment, alone. The two peptides together decreased the AP firing frequency ( $p = 0.03$ ), increased the inter-spike interval ( $p = 0.04$ ), and caused a marked increase of rheobase ( $p = 0.03$ ). All measured active and passive membrane parameters are presented in Table 2.

To determine whether the observed effects of peptide treatments were exerted directly on the POMC neurons, the experiments were repeated in the presence of TTX, an inhibitor of the  $\text{Na}^+$ -dependent action potentials. Treatment of slices with TRH (1  $\mu$ M; and 5  $\mu$ M) did not have a significant effect on either measured parameter (Fig. 5, Table 3). Administration of UCN3 into the bath solution (100 nM) caused a significant depolarization of the membrane potential of the POMC neurons in the ARC (control:  $-40.7 \pm 1.5$  mV; UCN3 treated:  $-34.1 \pm 1.7$  mV,  $p = 0.002$ ). UCN3 treatment did not change the membrane resistance ( $R_{\text{input}}$ ;  $p = 0.66$ ) and the tau values ( $p = 0.17$ ). The highly selective corticotrophin-releasing factor type 2 receptor (CRFR<sub>2</sub>) antagonist, K41498 (1  $\mu$ M), completely prevented the depolarizing effect of UCN3, while the CRFR<sub>2</sub> antagonist, alone, had no significant effect (Fig. 5; Table 3), indicating that the effects of UCN3 were mediated by CRFR<sub>2</sub>. However, when TRH (1  $\mu$ M) was co-administered with UCN3 (100 nM), the UCN3-induced depolarization was completely prevented, and the co-treatment even caused a hyperpolarization of MP ( $p = 0.003$ ).

## Discussion

To determine whether TRH/UCN3 neurons located in the perifornical/BNST region regulate food intake via orexigenic and/or anorexigenic neurons in the ARC, the



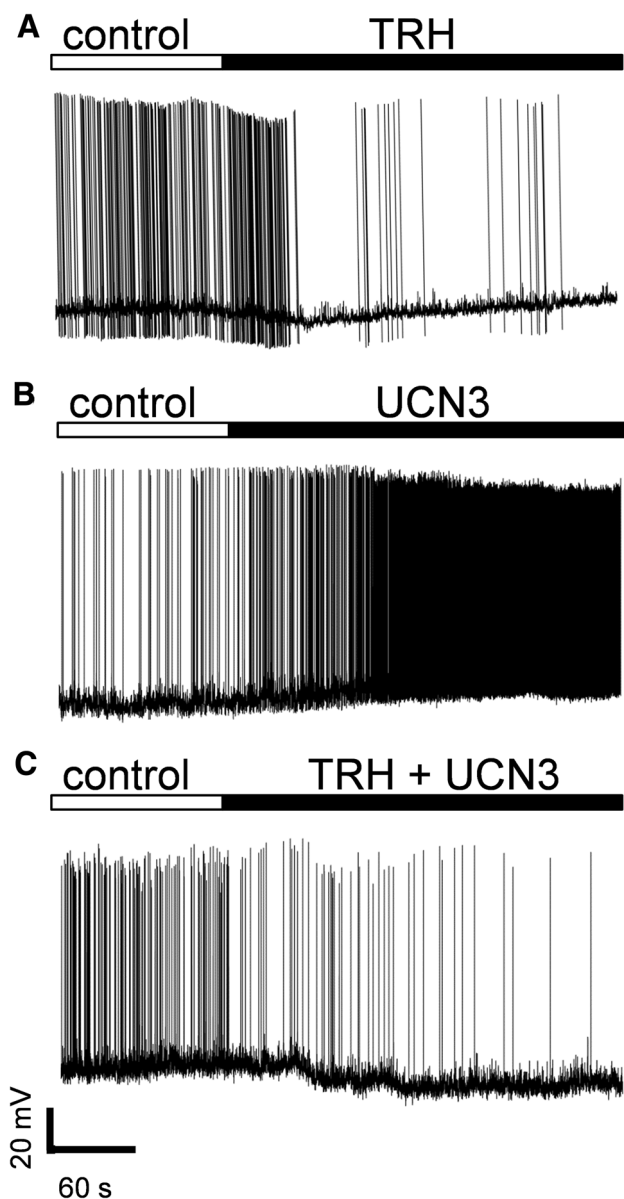


**Fig. 4** Sample recordings represent effects of TRH (1  $\mu$ M), UCN3 (100 nM), and the combination of the two peptides (TRH + UCN3) on spontaneous spike properties of the POMC neurons recorded in the arcuate nucleus

relationship between double-labeled TRH/UCN3 axons and the NPY or POMC neurons was studied in the ARC using triple-labeling immunofluorescence. The double-labeled axons contacted only a minority of NPY neurons, making it unlikely that TRH/UCN3 neurons have a major, direct influence on this orexigenic neuron population. We observed, however, that large number of single-labeled TRH-IR axons contacts the majority of NPY neurons, suggesting that TRH neurons that do not contain UCN3 may contribute to the regulation food intake via NPY neurons. This is supported by the finding of (Krashes et al. 2014) demonstrating that optogenetic stimulation of TRH

neurons in the PVN stimulates the NPY neurons of the ARC. However, it is unknown whether this effect is mediated by TRH or other transmitters that co-exist with TRH in TRH neurons such as glutamate (Hrabovszky et al. 2005).

In contrast, more than half of the anorexigenic POMC neurons were contacted by multiple TRH/UCN3 axon varicosities. Since the vast majority of UCN3 axons also contained TRH in the ARC, we used UCN3 as a marker of TRH/UCN3 fibers when the relationship of these axons and the POMC neurons were studied at the ultrastructural level. Double-labeling immuno-electron microscopy revealed that synaptic associations were frequently observed between the UCN3-IR axons and POMC-IR perikarya and dendrites. In all cases, the synaptic associations were asymmetric type, indicative of the excitatory nature of the synaptic communication.

To elucidate how TRH/UCN3 neurons regulate POMC neurons, the effects of TRH, UCN3, and the combination of these two peptides were studied on POMC neurons using electrophysiology. Since central administration of both TRH and UCN3 have a similar effect to reduce food intake as do activation of POMC neurons (Fekete et al. 2007; Lechan and Fekete 2006; Schwartz et al. 2000), we hypothesized that both peptides would stimulate POMC neurons and that their co-administration would have an additive effect. In contrast, the two peptides were observed to have opposite effects on POMC neurons. As expected, UCN3 markedly depolarized POMC neurons by acting on CRFR<sub>2</sub>, suggesting that UCN3 increases the excitability of these neurons. Indeed, UCN3 treatment markedly increased the spontaneous firing frequency of POMC neurons. TTX did not prevent the depolarizing effect of UCN3 suggesting that UCN3 exerts a direct stimulatory effect on POMC neurons. In contrast, TRH treatment caused hyperpolarization of POMC neurons and decreased the firing frequency of these cells. TTX treatment prevented the hyperpolarizing effect of TRH suggesting that the effect of TRH is at least partly mediated via other neurons innervating the POMC neurons. Simultaneous administration of TRH and UCN3 completely prevented the effects of UCN3 on the membrane potential and the firing of POMC neurons, indicating that while both peptides can act directly on POMC neurons, TRH antagonizes UCN3-induced stimulation rather than having an additive effect.

While TRH had no effect on the membrane resistance, UCN3 decreased this value independently from the presence of TRH in the bath solution. These data indicate that the activation of CRFR<sub>2</sub> by UCN3 induces the opening of ion channels in the membrane of POMC neurons. As TRH blocks the effect of UCN3 on the firing frequency but does not influence the effect of UCN3 on membrane resistance, one may conclude that TRH signaling interferes with

**Table 2** Comparison of the spontaneous spiking property and passive and active membrane properties of the POMC-expressing neurons in the ARC under different treatment conditions

	TRH		UCN3		TRH + UCN3	
	TRH		UCN3		TRH + UCN3	
	Control	TRH	Control	UCN3	Control	TRH + UCN3
Membrane potential (mV)	-45.75 ± 1.69 <i>p</i> = 0.0017	-49.44 ± 2.21; <i>n</i> = 10;	-50.37 ± 3.07	-43.73 ± 2.78; <i>n</i> = 9; <i>p</i> < 0.001	-43.15 ± 1.60	-47.32 ± 3.02; <i>n</i> = 10; <i>p</i> = 0.121
Spont. spike frequency (Hz)	1.54 ± 0.25	0.63 ± 0.18; <i>n</i> = 10; <i>p</i> = 0.009	0.64 ± 0.17	4.41 ± 0.82; <i>n</i> = 9; <i>p</i> < 0.001	1.42 ± 0.33	0.48 ± 0.19; <i>n</i> = 10; <i>p</i> = 0.024
Spont. spike amplitude (mV)	68.38 ± 5.38	68.63 ± 5.99; <i>n</i> = 10; <i>p</i> = 0.8	73.09 ± 4.60	69.17 ± 5.04; <i>n</i> = 9; <i>p</i> = 0.57	61.71 ± 2.84	61.59 ± 3.44; <i>n</i> = 10; <i>p</i> = 0.96
Membrane capacitance (pF)	25.87 ± 1.31	24.91 ± 1.23; <i>n</i> = 10; <i>p</i> = 0.31	27.07 ± 2.58	25.64 ± 2.7; <i>n</i> = 9; <i>p</i> = 0.41	28.48 ± 4.50	24.52 ± 2.00; <i>n</i> = 10; <i>p</i> = 0.2
Input resistance (MΩ)	866.91 ± 133.7	829.14 ± 11; <i>n</i> = 10; <i>p</i> = 0.49	1154.62 ± 191.47	857.49 ± 113.10; <i>n</i> = 9; <i>p</i> = 0.04	951.40 ± 124.8	728.27 ± 102.83; <i>n</i> = 10; <i>p</i> = 0.02
Membrane time constant (ms)	19.37 ± 1.56	16.72 ± 1.16; <i>n</i> = 10; <i>p</i> = 0.13	26.88 ± 3.41	20.35 ± 2.93; <i>n</i> = 9; <i>p</i> = 0.13	23.70 ± 1.96	17.55 ± 2.08; <i>n</i> = 10; <i>p</i> = 0.051
AP threshold (mV)	-26.11 ± 1.49	-27.41 ± 1.4; <i>n</i> = 10; <i>p</i> = 0.19	-25.18 ± 1.71	-26.50 ± 2.10; <i>n</i> = 9; <i>p</i> = 0.18	-20.85 ± 2.97	-20.11 ± 3.31; <i>n</i> = 10; <i>p</i> = 0.46
AP frequency max. (Hz)	32.99 ± 4.16	25.24 ± 5.31; <i>n</i> = 10; <i>p</i> = 0.01	33.83 ± 5.06	39.77 ± 4.36; <i>n</i> = 9; <i>p</i> = 0.005	21.10 ± 2.31	15.23 ± 3.70; <i>n</i> = 10; <i>p</i> = 0.03
Inter-spike interval (ms)	36.45 ± 6.49	54.68 ± 10.3; <i>n</i> = 10; <i>p</i> = 0.04	40.09 ± 10.79	30.51 ± 4.26; <i>n</i> = 9; <i>p</i> = 0.27	53.64 ± 6.50	104.53 ± 24.13; <i>n</i> = 10; <i>p</i> = 0.04
AP accommodation ratio	0.56 ± 0.06	0.60 ± 0.09; <i>n</i> = 10; <i>p</i> = 0.43	0.57 ± 0.08	0.86 ± 0.04; <i>n</i> = 9; <i>p</i> = 0.01	0.46 ± 0.04	0.41 ± 0.06; <i>n</i> = 10; <i>p</i> = 0.45
Rheobase (pA)	16.34 ± 4.15	26.73 ± 5.76; <i>n</i> = 10; <i>p</i> = 0.03	19.18 ± 3.77	11.28 ± 3.52; <i>n</i> = 9; <i>p</i> < 0.001	23.61 ± 3.94	47.95 ± 10.45; <i>n</i> = 10; <i>p</i> = 0.03
AP amplitude (mV)	55.74 ± 1.64	53.70 ± 1.55; <i>n</i> = 10; <i>p</i> = 0.07	52.42 ± 2.87	50.97 ± 3.81; <i>n</i> = 9; <i>p</i> = 0.28	51.36 ± 3.24	52.29 ± 2.70; <i>n</i> = 10; <i>p</i> = 0.83
AP half-width (ms)	0.66 ± 0.05	0.68 ± 0.04; <i>n</i> = 10; <i>p</i> = 0.53	0.78 ± 0.04	0.87 ± 0.05; <i>n</i> = 9; <i>p</i> = 0.02	0.72 ± 0.03	0.69 ± 0.03; <i>n</i> = 10; <i>p</i> = 0.47
Rise time 10–90 (ms)	0.24 ± 0.02	0.27 ± 0.03; <i>n</i> = 10; <i>p</i> = 0.10	0.27 ± 0.01	0.31 ± 0.02; <i>n</i> = 9; <i>p</i> = 0.02	0.28 ± 0.01	0.29 ± 0.02; <i>n</i> = 10; <i>p</i> = 0.36
Time to peak (ms)	0.32 ± 0.03	0.37 ± 0.03; <i>n</i> = 10; <i>p</i> = 0.31	0.37 ± 0.02	0.41 ± 0.03; <i>n</i> = 9; <i>p</i> = 0.09	0.30 ± 0.01	0.30 ± 0.01; <i>n</i> = 10; <i>p</i> = 0.88
AHP amplitude (mV)	-25.76 ± 1.63	-25.57 ± 1.7; <i>n</i> = 10; <i>p</i> = 0.79	-23.55 ± 1.53	-20.53 ± 1.27; <i>n</i> = 9; <i>p</i> = 0.05	-20.97 ± 1.51	-21.58 ± 2.07; <i>n</i> = 10; <i>p</i> = 0.56

Treatment conditions are as follows: TRH (1 μM), UCN3 (100 nM), and TRH + UCN3 (1 μM + 100 nM, respectively). Paired *t* test *p* values are in the treatment columns. All data are shown as mean ± SEM

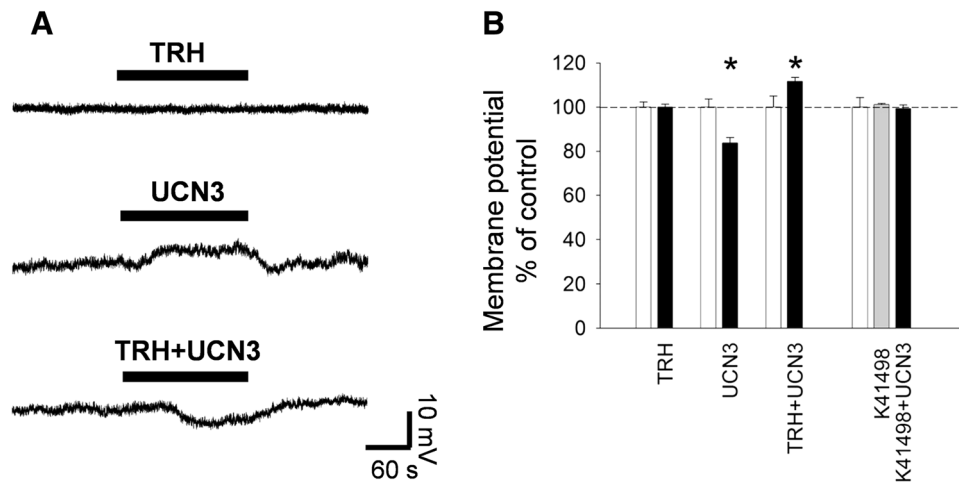


**Fig. 5** Effects of TRH, UCN3, and combination of the two peptides on the membrane potential of POMC neurons in the arcuate nucleus. Sample traces (a) illustrate the effects TRH (1  $\mu$ M), UCN3 (100 nM) and the combination of the two peptides. Bar graph (b) summarizes the results of membrane potential changes in the different

experimental groups. Data are presented as percentages of control values. White bars represent the control values, black bars represent the treatment values (TRH,  $n = 15$ ; UCN3,  $n = 10$ ; TRH + UCN3,  $n = 8$ ), and gray bar represents the CRFR<sub>2</sub> antagonist (K41498,  $n = 9$ ) treatment alone. Data are shown as mean  $\pm$  SEM, \* $p < 0.05$

**Table 3** Summary of the passive electrophysiological properties of synaptically isolated POMC-expressing neurons under different experimental conditions

Experimental conditions		MP (mV)	$R_{input}$ (M $\Omega$ )	Tau (ms)
TRH	CONTROL	$-41.47 \pm 0.99$ ; $n = 15$	$1177.31 \pm 179.80$ ; $n = 15$	$30.28 \pm 4.27$ ; $n = 15$
	TRH	$-41.44 \pm 0.10$ ; $n = 15$	$1026.54 \pm 140.49$ ; $n = 15$	$26.53 \pm 2.88$ ; $n = 15$
UCN3	CONTROL	$-40.66 \pm 1.48$ ; $n = 10$	$948.34 \pm 77.45$ ; $n = 10$	$24.02 \pm 3.50$ ; $n = 10$
	UCN3	$-34.11 \pm 1.71$ ; $n = 10^*$	$905.80 \pm 98.18$ ; $n = 10$	$18.66 \pm 1.38$ ; $n = 10$
TRH + UCN3	CONTROL	$-40.08 \pm 2.05$ ; $n = 8$	$991.50 \pm 105.49$ ; $n = 8$	$24.93 \pm 1.92$ ; $n = 8$
	TRH + UCN3	$-44.47 \pm 2.39$ ; $n = 8^*$	$759.20 \pm 94.57$ ; $n = 8$	$18.19 \pm 1.69$ ; $n = 8$
K41498 + UCN3	CONTROL	$-44.12 \pm 1.95$ ; $n = 9$	$728.05 \pm 90.58$ ; $n = 9$	$15.39 \pm 1.39$ ; $n = 9$
	K41498	$-44.66 \pm 2.08$ ; $n = 9$	$643.74 \pm 81.08$ ; $n = 9$	$13.67 \pm 1.48$ ; $n = 9$
	K41498 + UCN3	$-44.19 \pm 1.90$ ; $n = 9$	$639.22 \pm 103.50$ ; $n = 9$	$13.93 \pm 1.66$ ; $n = 9$

The measured parameters are as follows: membrane potential (MP), input resistance ( $R_{input}$ ), and membrane time constant (Tau). Data were recorded in the presence of TTX (660 nM). All data are shown as mean  $\pm$  SEM, \* $p < 0.05$

UCN3 signaling at the level of second messengers, downstream of ion channel opening.

The lack of a TRH-induced effect on the membrane potential of POMC neurons and the antagonistic effect of the two peptides was surprising, as TRH has stimulatory effects on many cell types (Ishibashi et al. 2009; Zhang et al. 2013; Hara et al. 2009). However, Ballerini et al. (Ballerini et al. 1994) observed a similar phenomenon in pyramidal cells of the hippocampal CA1 region, showing that TRH has no effect on the membrane potential of those cells but prevented the effect of an other transmitter (Ballerini et al. 1994). The highly divergent effects of TRH on target neurons may be due to differential expression of the two, TRH receptors, TRHR1 and 2, in these cell populations. Since specific antagonists of TRH receptors are unavailable, the receptor specificity of the TRH effect on

POMC neurons could not be tested. While both types of TRH receptors are expressed in the ARC (Heuer et al. 2000), data is not currently available as to which of the TRH receptors are present in POMC neurons.

While UCN3 may inhibit food intake by stimulating POMC neurons of the ARC, these data suggest that TRH may prevent or terminate the effect of UCN3. These data are especially interesting because the two, anorexigenic peptides are released from the very same axon terminals, yet exert antagonistic effects on the POMC neurons. So far, the physiological importance of this interaction is not yet clear. We hypothesize, however, that the differential expression and release of the two peptides enables TRH/UCN3 neurons to exert distinct effects on the POMC neurons under different physiological or pathophysiological conditions. Further studies using optogenetics may help

to understand whether the length, pattern or the frequency of the firing of TRH/UCN3 neurons differentially alters the release of the two peptides, and whether the two peptides are released simultaneously, independently or sequentially from the same axons. In the latter case, TRH might have a role to terminate the UCN3-induced excitation of POMC neurons.

In addition to the TRH/UCN3 axons, a large number of single-labeled TRH axons were observed in juxtaposition to the POMC neurons. Therefore, TRH released from these non-UCN3 axon terminals may also modify the effect of the UCN3 on the POMC neurons. The source and function of these TRH axons are currently unknown.

Since stress increases the synthesis of UCN3 in perifornical neurons (Liu et al. 2007) and causes anorexia via activation of the POMC neurons of the ARC (Liu et al. 2007). Thus, based on our current data, we raise the possibility that TRH/UCN3 neurons of the perifornical area/BNST region mediate the effects of stress on POMC neurons. Still, further studies are necessary to understand the importance of this pathway in the stress-induced activation of the POMC neurons and to identify the pathways activating the TRH/UCN3 neurons during stress.

In summary, these studies demonstrate that the TRH/UCN3 neurons establish synaptic associations with POMC neurons of the ARC, and unveil a novel antagonistic effect of the two peptides in the regulation of these neurons. These data support the hypothesis that TRH/UCN3 neurons of the perifornical area/BNST region may be involved in stress-induced activation of anorexigenic POMC neurons.

**Acknowledgements** This work was supported by Grants from the Hungarian Science Foundation (OTKA K109710) and the Hungarian National Brain Research Program (KTIA\_13\_NAP\_A\_I/3).

**Author contributions** ZP performed the electrophysiological experiments. EF were involved in the immunofluorescent studies, performed the immunostaining in mice, did the electron microscopy and were involved in the generation of the two novel antibodies. KN performed the first immunofluorescent studies and performed the quantitative analyses under the supervision of TF. AK were involved in the immunofluorescent studies. OS and AH were involved in the generation of the two novel antibodies. RML: data interpretation, manuscript preparation; CF: Experimental design, data acquisition, drafting, revising and interpretation of the work, takes primary responsibility.

**Compliance with ethical standards**

**Conflict of interest** The authors have nothing to disclose.

## References

- Ballerini L, Corradetti R, Nistri A, Pugliese AM, Stocca G (1994) Electrophysiological interactions between 5-hydroxytryptamine and thyrotropin releasing hormone on rat hippocampal CA1 neurons. *Eur J Neurosci* 6(6):953–960
- Elias CF, Saper CB, Maratos-Flier E, Tritos NA, Lee C, Kelly J, Tatro JB, Hoffman GE, Ollmann MM, Barsh GS, Sakurai T, Yanagisawa M, Elmquist JK (1998) Chemically defined projections linking the mediobasal hypothalamus and the lateral hypothalamic area. *J Comp Neurol* 402(4):442–459
- Fekete C, Lechan RM (2014) Central regulation of hypothalamic-pituitary-thyroid axis under physiological and pathophysiological conditions. *Endocr Rev* 35(2):159–194. <https://doi.org/10.1210/er.2013-1087>
- Fekete EM, Inoue K, Zhao Y, Rivier JE, Vale WW, Szucs A, Koob GF, Zorrilla EP (2007) Delayed satiety-like actions and altered feeding microstructure by a selective type 2 corticotropin-releasing factor agonist in rats: intra-hypothalamic urocortin 3 administration reduces food intake by prolonging the post-meal interval. *Neuropsychopharmacology* 32(5):1052–1068. <https://doi.org/10.1038/sj.npp.1301214>
- Gropp E, Shanabrough M, Borok E, Xu AW, Janoschek R, Buch T, Plum L, Balthasar N, Hampel B, Waisman A, Barsh GS, Horvath TL, Bruning JC (2005) Agouti-related peptide-expressing neurons are mandatory for feeding. *Nat Neurosci* 8(10):1289–1291. <https://doi.org/10.1038/nn1548>
- Hara J, Geraschenko D, Wisor JP, Sakurai T, Xie X, Kilduff TS (2009) Thyrotropin-releasing hormone increases behavioral arousal through modulation of hypocretin/orexin neurons. *J Neurosci* 29(12):3705–3714. <https://doi.org/10.1523/JNEUROSCI.0431-09.2009>
- Heuer H, Schafer MK, O'Donnell D, Walker P, Bauer K (2000) Expression of thyrotropin-releasing hormone receptor 2 (TRH-R2) in the central nervous system of rats. *J Comp Neurol* 428(2):319–336
- Hrabovszky E, Wittmann G, Turi GF, Liposits Z, Fekete C (2005) Hypophysiotropic thyrotropin-releasing hormone and corticotropin-releasing hormone neurons of the rat contain vesicular glutamate transporter-2. *Endocrinology* 146(1):341–347. <https://doi.org/10.1210/en.2004-0856>
- Ishibashi H, Nakahata Y, Eto K, Nabekura J (2009) Excitation of locus coeruleus noradrenergic neurons by thyrotropin-releasing hormone. *J Physiol* 587(Pt 23):5709–5722. <https://doi.org/10.1113/jphysiol.2009.181420>
- Krashes MJ, Shah BP, Madara JC, Olson DP, Strohlic DE, Garfield AS, Vong L, Pei H, Watabe-Uchida M, Uchida N, Liberles SD, Lowell BB (2014) An excitatory paraventricular nucleus to AgRP neuron circuit that drives hunger. *Nature* 507(7491):238–242. <https://doi.org/10.1038/nature12956>
- Lechan RM, Fekete C (2006) The TRH neuron: a hypothalamic integrator of energy metabolism. *Prog Brain Res* 153:209–235
- Liu J, Garza JC, Truong HV, Henschel J, Zhang W, Lu XY (2007) The melanocortinergic pathway is rapidly recruited by emotional stress and contributes to stress-induced anorexia and anxiety-like behavior. *Endocrinology* 148(11):5531–5540. <https://doi.org/10.1210/en.2007-0745>
- Luquet S, Perez FA, Hnasko TS, Palmiter RD (2005) NPY/AgRP neurons are essential for feeding in adult mice but can be ablated in neonates. *Science* 310(5748):683–685. <https://doi.org/10.1126/science.1115524>
- Sarvari A, Farkas E, Kadar A, Zseli G, Fuzesi T, Lechan RM, Fekete C (2012) Thyrotropin-releasing hormone-containing axons innervate histaminergic neurons in the tuberomammillary nucleus. *Brain Res* 1488:72–80. <https://doi.org/10.1016/j.brainres.2012.10.010>
- Schwartz MW, Woods SC, Porte D Jr, Seeley RJ, Baskin DG (2000) Central nervous system control of food intake. *Nature* 404(6778):661–671. <https://doi.org/10.1038/35007534>

- Wittmann G, Liposits Z, Lechan RM, Fekete C (2002) Medullary adrenergic neurons contribute to the neuropeptide Y-ergic innervation of hypophysiotropic thyrotropin-releasing hormone-synthesizing neurons in the rat. *Neurosci Lett* 324(1):69–73
- Wittmann G, Fuzesi T, Liposits Z, Lechan RM, Fekete C (2009) Distribution and axonal projections of neurons coexpressing thyrotropin-releasing hormone and urocortin 3 in the rat brain. *J Comp Neurol* 517(6):825–840. <https://doi.org/10.1002/cne.22180>
- Wittmann G, Hrabovszky E, Lechan RM (2013) Distinct glutamatergic and GABAergic subsets of hypothalamic pro-opiomelanocortin neurons revealed by in situ hybridization in male rats and mice. *J Comp Neurol* 521(14):3287–3302. <https://doi.org/10.1002/cne.23350>
- Zhang L, Kolaj M, Renaud LP (2013) GIRK-like and TRPC-like conductances mediate thyrotropin-releasing hormone-induced increases in excitability in thalamic paraventricular nucleus neurons. *Neuropharmacology* 72:106–115. <https://doi.org/10.1016/j.neuropharm.2013.04.023>